Portable Document Format (.pdf) Reproduction

Journal of ELECTRONIC MATERIALS

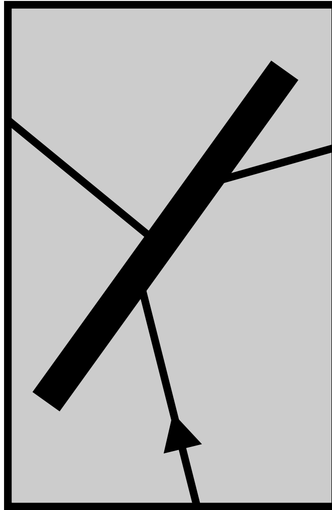

May 1999

"Temperature Dependent Optical Properties of Self-Organized InAs/GaAs Quantum Dots"

Reprinted from JEM, *Vol. 28 No. 5, May 1999, pp. 520–527.*

Temperature Dependent Optical Properties of Self-Organized InAs/GaAs Quantum Dots

R. HEITZ,[1,2] I. MUKHAMETZHANOV,[3] A. MADHUKAR,[3] A. HOFFMANN,[1] and D. BIMBERG[1]

1.—Institut für Festkörperphysik, Technische Universität Berlin, Berlin, Germany. 2.—e-mail: heitz@sol.physik.tu-berlin.de. 3.—Photonic Materials and Devices Laboratory, University of Southern California, Los Angeles, CA 90089-0241

We report photoluminescence (PL), time-resolved PL, and PL excitation experiments on InAs/GaAs quantum dots (QDs) of different size as a function of temperature. The results indicate that both the inhomogeneous properties of the ensemble and the intrinsic properties of single QDs are important in understanding the temperature-dependence of the optical properties. With increasing temperature, excitons are shown to assume a local equilibrium distribution between the localized QD states, whereas the formation of a position-independent Fermi-level is prevented by carrier-loss to the barrier dominating thermally stimulated lateral carrier transfer. The carrier capture rate is found to decrease with increasing temperature and, at room temperature, long escape-limited ground state lifetimes of some 10 ps are estimated. PL spectra excited resonantly in the ground state transition show matching ground state absorption and emission, indicating the intrinsic nature of exciton recombination in the QDs. Finally, the PL excitation spectra are shown to reveal size-selectively the QD absorption, demonstrating the quantum-size effect of the excited state splitting.

Key words: InAs/GaAs, photoluminescence excitation spectroscopy, self-organized quantum dots (QDs)

INTRODUCTION

The formation of nanoscale coherent islands in highly strained semiconductor epitaxy has been extensively studied as means to generate optically active quantum dots (QDs).[1] In spite of the large size inhomogeneity[2–5] of ~10% and the interdependent nature of the QD density and size, such Stranski-Krastanow QDs have been successfully employed in devices.[6,7] The inhomogeneous broadening of the discrete density of states for the self-organized QD ensembles hampers detailed investigations of the excited state spectrum and of energy relaxation (and recombination) processes, which are both of basic physical interest and critical for design and performance of devices. In fact, it is often necessary to distinguish between ensemble effects and the properties of single QDs.

The properties of an ensemble of non-interacting QDs cannot be described by a common Fermi-level, but are governed by statistical feeding of independent QDs.[8,9] For single QDs, the predicted slow-down of carrier relaxation processes[10] might also prevent an equilibrium population of electronic states. Some experimental work has, thus, been devoted to the study of the temperature dependence of the QD photoluminescence (PL) and its dynamical behavior.[6,11–19] With increasing temperature, lateral exciton transfer via the wetting layer (WL) has been argued to lead to a redistribution of the exciton population favoring larger QDs in the ensemble.[15,16] Such lateral coupling is a possible means for the formation of a common Fermi-level. Here we present temperature-dependent PL and PL excitation (PLE) measurements for two types of samples with different QD ground state transition energy and full width at half maximum (FWHM), signifying different average size and uniformity of the QD ensembles. The temperature-dependence of the optical QD properties is shown to depend on the inhomogeneous properties of QDs in the ensemble as well as on the intrinsic

(Received December 15, 1998; accepted January 5,1999)

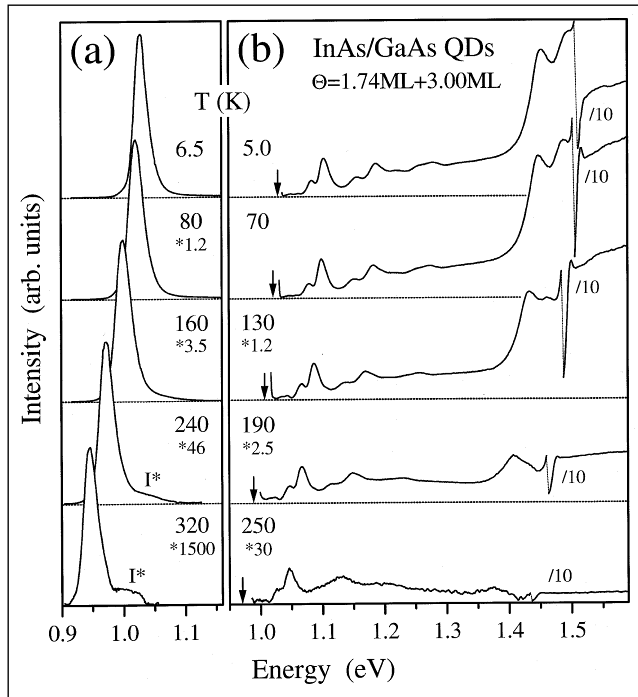

Fig. 1. PL (a) and PLE (b) spectra for the 3.00 ML sample at various temperatures. The PL spectra were excited with an Ar^+ laser at an excitation density of $5 Wcm^{-2}$. The excitation density for the PLE experiments was <0.02 Wcm^{-2}. The detection energies of the PLE spectra are indicated by arrows in panel (b).

properties of single QDs. The decreasing PL yield with increasing temperature for nonresonant excitation is attributed to a decreasing excitation efficiency and not, as often assumed, thermally induced escape of carriers from the ground state. The results exclude significant lateral carrier transfer between QDs for temperatures up to 250K and, therewith, the formation of a common Fermi-level. Excitons are shown, however, to assume a local equilibrium state population in single QDs, allowing the observation of size-selective ground state absorption in PLE spectra of excited state transitions. Finally, PLE spectra are shown to reveal the excited state absorption spectrum in the investigated samples. This is remarkable since PLE spectra have been controversially discussed in the framework of excited state absorption[4,19] and carrier relaxation processes leading to multi-phonon resonances.[18,20,21]

EXPERIMENTAL

The two investigated InAs/GaAs QD samples were grown by molecular beam epitaxy on semi-insulating GaAs(001) substrates. InAs was deposited at 500°C, an As_4 partial pressure of 6×10^{-6} Torr, and a growth rate of 0.22 MLs^{-1} as described in Refs. 4 and 22. The InAs layers were capped at 400°C using migration enhanced epitaxy (MEE).[4] The first sample consists of a single layer with 1.74 ML InAs deposition. The second sample is a bilayer sample with a 1.74 ML seed layer and a 3.00 ML second layer separated by a 36 ML MEE-grown GaAs spacer. This variable deposition amount approach[22] enables independent control of the QD density and size and improves the uniformity of the QD ensemble. In such samples, vertical pairs of a small QD in the seed layer and a larger one in the second layer are formed. Luminescence is observed only from QDs in the second layer due to efficient energy transfer processes from the seed layer.[23] AFM investigations for identically grown uncapped samples yield a QD density of 3.8×10^{10} cm^{-2} {4.8×10^{10} cm^{-2}}, an average height of (38±9)Å {(97±7)Å}, and an average width of (169±18)Å {(256±12)Å} for the 1.74 ML {3.00 ML} sample.[22] The QDs are located on top of an ~1 ML thick WL with a transition energy of ~1.455 eV.[23]

The samples were mounted in a continuous-flow He-cryostat, providing temperatures between 3.5 and 360K. PL was excited either by an Ar^+ laser or a tungsten lamp dispersed by a 0.27 m double-grating monochromator as tunable, low excitation density (<0.02 Wcm^{-2}) light source. The PL was dispersed in a double-grating monochromator and detected by a cooled Ge-diode (North Coast 817 L). Time-resolved PL was excited by 6 ps pulses of a synchronously pumped dye-laser at 670 nm in the GaAs barrier, dispersed by a 0.35 m subtractive double-grating monochromator, and detected with a multi-channel plate photomultiplier with a S1-cathode in photon-counting mode. The system response with a FWHM of ~50 ps was taken into account in the analysis of the transients.

EXPERIMENTAL RESULTS AND DISCUSSION

He-temperature PL spectra of the 1.74 and 3.00 ML samples have been reported in Ref. 22. Both samples show at low excitation densities only a single PL peak attributed to the QD ground state transition. For the 1.74 ML sample the PL peak is centered at 1.175 eV and has a FWHM of 75 meV. For the 3.00 ML sample, the larger island size and improved uniformity of the islands result in a lower transition energy (1.028 eV) and a smaller FWHM of only 25 meV, respectively. The significantly different carrier confinement with respect to the WL, amounting in average to 270 and 430 meV, respectively, should reflect in activation energies deduced from the temperature dependence of the optical properties.

Figure 1 depicts PL (a) and PLE (b) spectra for the 3.00 ML sample for various temperatures. (Note that PL and PLE spectra have been taken at different temperatures.). With increasing temperature, the QD PL shifts toward lower energies, almost maintaining its shape until above ~200K a high-energy shoulder indicates thermal population of excited states (I*). The PLE spectra recorded on the (temperature-dependent) PL maximum (the detection energies are marked by arrows in panel (b)) reveal different excitation channels: These are *nonresonant* excitation via capture of carriers or excitons from the GaAs barrier (scaled down in Fig. 1b by a factor of 10) or the WL and, at lower energies, *localized (near-resonant)* excitation via excited state transitions of the QDs. In the lattermost case one carrier might be

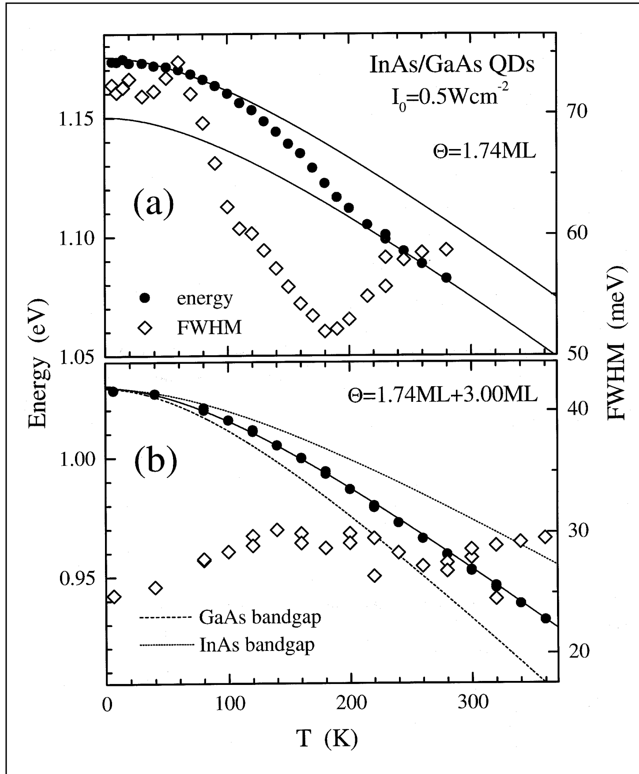

Fig. 2. FWHM (diamonds) and energy (dots) of the ground state transition of the QDs in the 1.74 ML (a) and the 3.00 ML (b) sample as a function of temperature. The temperature change of the bulk InAs and GaAs bandgaps is depicted by the dotted and dashed lines in panel (b), respectively. Full lines show the variation of the QD ground state transition energy in the 3.00 ML sample fitted with the Varshni formula.

excited into the WL or GaAs barrier and efficiently recaptured by the charged QD. The distinct resonances observed close to the detection energy are attributed to excited state transitions of the QDs. However, it has been shown that the actual appearance of the near-resonant PLE spectra depends on the sample properties, i.e., the uniformity of the QD ensemble[19] as well as intrinsic or extrinsic recombination channels that compete with carrier relaxation.[18,21] Below, we will demonstrate that for the 3.00 ML sample, the PLE spectra indeed follow the absorption spectrum and, changing the detection energy, reveal the size-dependent excited state spectrum. With increasing temperature, nonresonant excitation of the QDs via the GaAs barrier and the WL becomes less efficient, whereas near-resonant excitation maintains its efficiency up to ~200K, indicating the carrier capture efficiency to limit the PL yield upon nonresonant excitation. Above ~200K, at least carriers in excited QD states are also thermally evaporated, quenching the PL yield for near-resonant excitation, too.

Figure 2 depicts the energy (dots) and FWHM (diamonds) of the QD ground state transition for the 1.74 ML (a) and 3.00 ML (b) samples as a function of temperature, demonstrating qualitatively different behaviors. For the 1.74 ML sample, the FWHM decreases by ~30% above ~80K and the ground state transition energy shows an accompanying low-energy shift of the transition energy. This behavior is an ensemble effect and has been attributed to preferential quenching of luminescence from the smaller QDs, which provide less carrier localization.[15,16] Such preferential quenching is obviously negligible for the 3.00 ML sample, for which the FWHM increases slightly for temperatures up to ~120K and the ground state transition shifts smoothly to lower energies. The relative inhomogeneous broadening of the exciton localization energy is much smaller for the 3.00 ML (5.8%) sample than for the 1.74 ML sample (27%), rendering ensemble effects negligible. Thus, for the 3.00 ML sample the temperature evolution of the transition energy and the FWHM are likely to be dominated by intrinsic properties of the QDs. The slight increase of the FWHM from 25 to 30 meV below ~120K might be attributed to the thermal population of excited hole states expected a few meV above the ground state.[24] We note that the low-energy slope of the QD PL peak maintains its shape (see Fig. 5a for a semilogarithmic plot) showing inhomogeneous broadening to dominate the lineshape for temperatures up to 360K. Fits of a Voigt profile, centered in the peak maximum, to the low energy slope place an upper limit of ~4 meV on the FWHM of the Lorentz contribution for temperatures up to 360K. The Lorentz contribution describes the homogeneous line profile of the single QDs. At temperatures below 50K, FWHMs of less than 150 μeV have been reported for single QD PL.[25,26] Phonon scattering processes are, however, expected to cause much larger homogeneous FWHMs at higher temperatures.

The temperature-dependent energy shift of bulk bandgaps is phenomenologically described by the Varshni's formula[27]

$$\Delta E = \frac{A \cdot T^2}{T + B}, \tag{1}$$

with A and B being parameters characteristic for the semiconductor. The full line in Fig. 2b represents a fit of Eq. (1) to the temperature-dependent line position. The experimental data for the 3.00 ML sample are well described with A = 0.00042 eVK^{-2} and B = 199K. The temperature evolution of the ground state transition energy falls in between of that of the bulk InAs (dotted line) and GaAs (dashed line) bandgaps, which are expected to be the limiting behavior for large and small QDs, respectively. The ensemble effects observed for the 1.74 ML sample make a fit of the transition energy with Eq. (1) meaningless. The parameters obtained for the 3.00 ML sample describe, however, reasonably well the ground state transition energy in the 1.74 ML sample in both the low and high temperature regions (full lines in Fig. 2a). The energy offset of 25 meV is, however, larger than the decrease of the FWHM (~21 meV), suggesting that the temperature-dependence of the ground state transition energy is indeed steeper in the 1.74 ML sample than in the 3.00 ML sample. The weaker localization of the electron and hole wavefunctions in the smaller QDs leads to a more GaAs-like behavior. A detailed

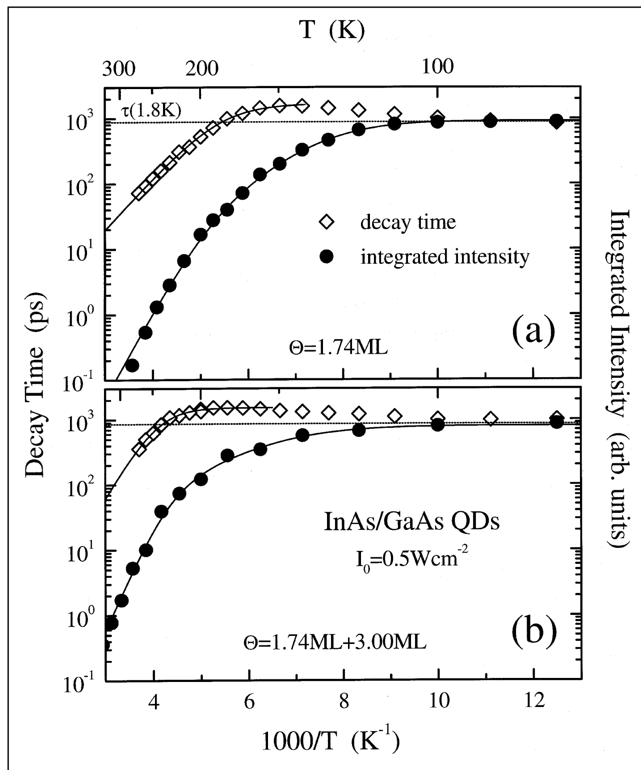

Fig. 3. Temperature-dependence of the PL decay time (diamonds) and the integrated PL intensity (dots) for the 1.74 ML (a) and the 3.00 ML (b) sample. The horizontal dotted lines indicate the ground state decay time at 1.8K, being (790±50) and (840±50) ps, respectively. Full lines show fits to the high temperature decreases of the decay time and the integrated intensity assuming one and two thermally activated nonraditive recombination processes, respectively.

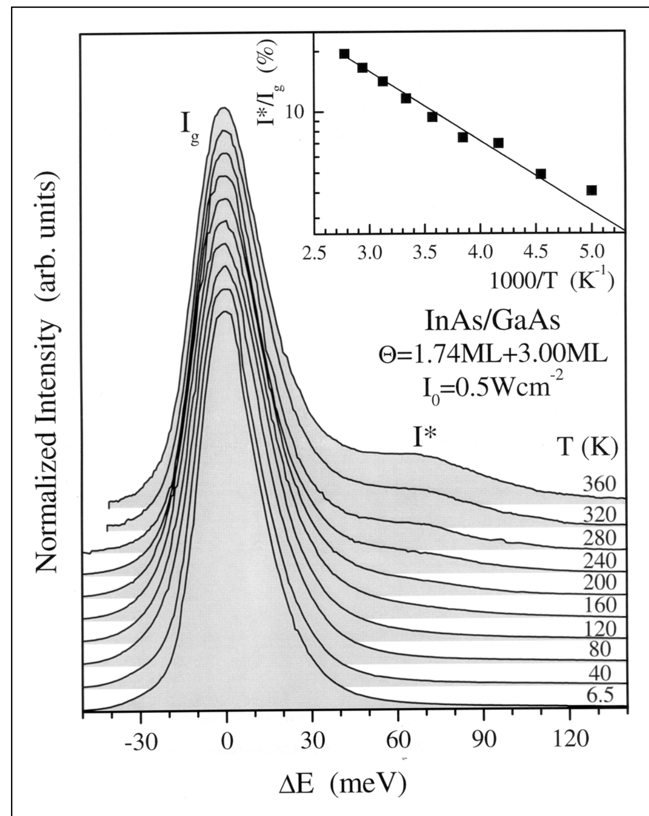

Fig. 4. PL spectra of the 3.00 ML sample for various temperatures. The spectra are normalized and plotted with respect to the respective peak energy for a comparison of the lineshapes. The insert shows the ratio (I^*/I_g) of the integrated intensities of the excited and the ground state PL transitions on a semilogarithmic scale.

understanding of the temperature-dependence of the ground state transition energy would require numerical calculations with temperature-dependent material parameters.

Dots in Fig. 3 depict the temperature evolution of the integrated QD PL intensity for the 1.74 ML (panel (a)) and 3.00 ML (panel (b)) samples. The intensity begins to decrease above ~100K in good agreement with the onset of preferential quenching observed for the 1.74 ML sample. Above ~200K, the intensity-decrease becomes steeper. In order to obtain satisfactory fits of the integrated intensity I (solid lines in Fig. 3), we had to assume two thermally activated nonradiative recombination processes with activation energies E_1 and E_2 to compete with radiative recombination, giving[28]

$$I \sim \frac{1}{1 + B_1 \cdot \exp(-E_1 / kT) + B_2 \cdot \exp(-E_2 / kT)}. \quad (2)$$

The comparatively soft decrease between 100 and 200K corresponds to activation energies of (110±20) and (75±15) meV, and the steep decay above ~200K corresponds to (270±50) and (320±40) meV for the 1.74 and 3.00 ML samples, respectively. For both samples, the energy E_1 is close to the respective excited state splitting observed in high-density or room-temperature PL experiments (see e.g., Fig. 4) and E_2 is close to the localization energy of the ground state exciton with respect to the WL. Thus, the two nonradiative processes could tentatively be assigned to thermally induced exciton escape out of the ground and an excited state of the QDs. Thereby, the large values of B_i obtained in the fits suggest the nonradiative recombination probability in the barrier to dominate recapture. We stress, however, that this comparatively simple interpretation is most likely incorrect. First, calculations[24] as well as PLE experiments (see below) indicate a significantly denser excited state transition spectrum than suggested by nonresonantly excited PL experiments. Thus, a variety of excited state transitions should contribute to E_1. Secondly, the exciton binding energy in the InAs/GaAs QDs is of the order of 20 meV[24] and, thus, considerably smaller than the carrier localization and quatization energies. Since the escape of one carrier already quenches the PL, one should expect to observe single carrier activation energies. Finally, the PLE spectra of the 3.00 ML sample shown in Fig. 1b unambiguously demonstrate a stronger quenching of the excitation efficiency for nonresonant (GaAs and WL) compared to near-resonant excitation, showing a decreasing excitation efficiency to contribute to the quenching of the PL intensity upon nonresonant excitation. A similar behavior has been observed for smaller QDs, too.[19]

This effect becomes quite obvious when comparing

the integrated PL intensity with the lifetime of the ground state exciton, diamonds in Fig. 3. Below ~100K, the PL decay time is practically independent of temperature and QD size, being (790±50) and (840±50) ps, respectively, for the 1.74 ML (panel (a)) and the 3.00 ML (panel(b)) sample. The dotted horizontal lines indicate the lifetime observed at 1.8K. Above ~100K, the lifetime increases up to ~1600 ps before it finally starts to decrease. The *radiative* recombination probability of a given exciton transition is temperature-independent, accounting for the constant lifetime at low temperatures. With increasing temperature, however, thermal population of excited states becomes important, resulting in an effective lifetime depending on the oscillator strength of the involved excited state transitions. Due to a smaller substate splitting, excited hole states will be populated first. The low probability of recombination between excited hole states and the electron ground state[24] thus explains the experimentally observed increase of the effective lifetime. Finally, thermally induced escape will dominate resulting in a decreasing exciton lifetime. Qualitatively similar results for smaller QDs with ~120 meV exciton localization have been successfully simulated considering one localized exciton state and delocalized WL states.[29] In the present case, however, a complete simulation is hampered by the need to include a spectrum of excited state transitions. Assuming a constant radiative lifetime τ_{rad} and that carriers activated into the barrier will recombine nonradiatively, the decrease of the lifetime at high temperatures is fitted by

$$\tau = \frac{\tau_{rad}}{1 + B \cdot \exp(-E_\tau / kT)}, \quad (3)$$

yielding activation energies E_τ of (170±30) and (240±30) meV, respectively, for the 1.74 and the 3.00 ML sample. These activation energies indicate thermal evaporation of single carriers to the WL to be the driving mechanism behind the decrease of the exciton lifetime. The estimated room temperature (300K) lifetimes of 35 and 150 ps are dominated by thermally induced escape. We note that Eq. (2) and Eq. (3) assume a constant radiative lifetime. As shown above, however, the effective radiative lifetime is temperature-dependent (see Fig. 3) due to the population of excited states. Thus, the determined activation energies have to be taken as estimates.

Mukai et al.[13] proposed thermally activated nonradiative recombination in the barrier to explain the decreasing excitation efficiency of their QD PL. The activation energies were thereby characteristic for the nonradiative recombination centers. The present experimental results, however, suggest the carrier capture probability itself to be temperature dependent, i.e. to decrease with increasing temperature. A possible reason might be the slowed-down carrier relaxation in QDs, allowing thermally induced escape to dominate intradot relaxation for carriers captured into excited states. Models taking into account a realistic electronic spectrum and the carrier dynamics in the QDs as well as in the GaAs barrier[13] are required to understand the temperature-dependent excitation efficiency. Finally, the decreasing FWHM of the QD PL observed for the 1.74 ML sample (Fig. 2a) has been taken as evidence for thermally induced lateral energy transfer via the WL.[15,16] Such lateral interaction of QDs could enable the formation of a position-independent Fermi-level at high temperatures, which would impact the carrier dynamics and, e.g., the characteristics of QD lasers.[8,9] Figure 1b shows for the 3.00 ML sample, however, that the PLE process remains size-selective even at temperatures (250K) well above the regime where lateral exciton transfer should become important. Carriers, which are thermally excited into the GaAs barrier, are subject to nonradiative recombination, favored with increasing temperatures by a decreasing carrier capture probability and an increasing nonradiative recombination probability.

Figure 4 depicts the QD PL peak in the 3.00 ML sample for temperatures up to 360K. The spectra are normalized and plotted via $\Delta E = E_{det} - E_{peak}$ for a comparison of the lineshapes. Above ~200K, the excited state transition I* becomes visible shifted 72 meV with respect to the ground state transition peak I_g. The ratio I^*/I_g of the integrated intensities of excited and ground state PL depends exponentially on the inverse temperature, as shown in the insert. A fit, assuming a three-level model and neglecting degeneracies, yields an activation energy of (70±5) meV and an oscillator strength ratio f^*/f_g of 1.7 in good agreement with the excited state splitting observed in nonresonantly excited PL and the predicted oscillator strengths.[24] Figure 4 demonstrates a local equilibrium distribution of carriers between ground and excited states of single QDs in the investigated InAs/GaAs QDs. The prediction of slowed down carrier relaxation and of a possible phonon-bottleneck effect for QDs[10] makes it necessary to verify the formation of a local equilibrium state experimentally.

The resolution in the nonresonantly excited PL experiments is limited by the inhomogeneous broadening, compare e.g., Fig. 4. The PLE spectra (Fig. 1b) suggest that, despite the remarkably low FWHM of 25 meV of the ground state transition in the 3.00 ML sample, the inhomogeneous FWHM masks additional finestructure. Figure 5a depicts for the 3.00 ML sample and T = 190K the nonresonantly excited PL (full line) and the PLE spectrum taken in a 3.4 meV window around the PL maximum at 0.990 eV on a semilogarithmic scale. The PL spectrum clearly shows the excited state transition I*, which has generally been attributed to the first excited state transition. The size-selective PLE spectrum reveals, however, a richer fine structure with I* corresponding to the most intense excitation resonance at 1.067 eV. The fine structure of the PLE spectra has been controversially discussed,[18,19,21] since carrier relaxation processes might produce fine structure in PLE spectra rendering an unambiguous identification of excited state transitions difficult. Here, we propose to take

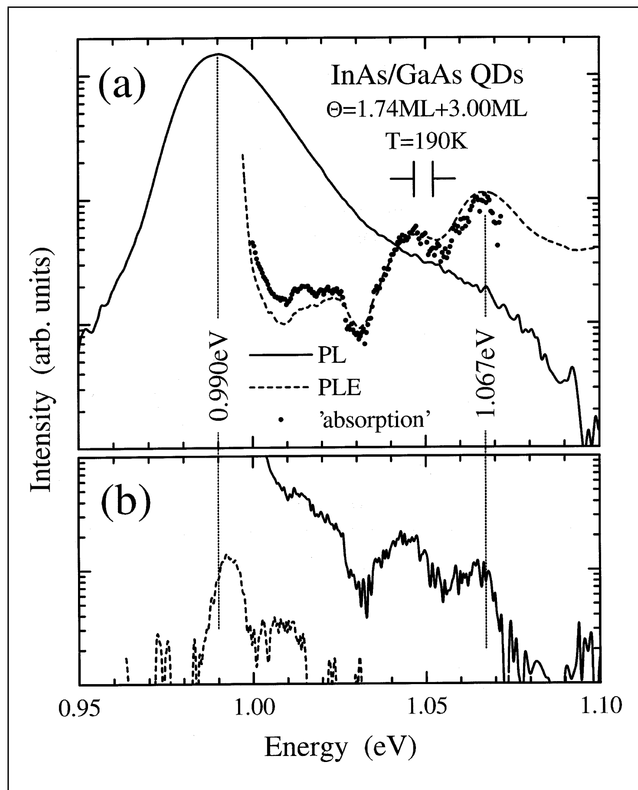

Fig. 5. PL (full lines) and PLE (dashed lines) spectra of the 3.00 ML sample at 190K. Panel (a) shows the nonresonantly excited PL as well as the PLE detected in the maximum of the PL spectrum. Panel (b) depicts spectra where the excitation energy was lower than the detection energy, necessitating subsequent excitation of photoexcited carriers into higher-energy states by phonon absorption. The PL spectrum was excited at 0.990 eV resonantly in the ground state transition and the PLE spectrum was detected at 1.067 eV on an excited state transition. The dots in panel (a) represent the "absorption" spectrum generated from the resonantly excited PL spectrum by multiplication with $\exp((E_{exc} - E_{det})/kT)$.

advantage of the *thermal population* of excited QD states upon *resonant excitation of the ground state* to investigate the ground state transition as well as the excited state spectrum of the QDs in more detail.

Panel (b) in Fig. 5 compares PL (full lines) and PLE (dashed lines) spectra where the excitation energy is smaller than the detection energy. Thus, photogenerated excitons have to additionally absorb phonons to reach excited states and, thus, to generate signal. Exciting resonantly in the center of the ground state transition (E_{exc} = 0.990 eV), weak structured luminescence is observed on the *high-energy* side (full line). The various PL lines are attributed to recombination between thermally populated excited states of the subensemble of QDs excited size-selectively in the ground state. The PLE spectrum detected at 1.067 eV on an excited state transition reveals the ground state absorption at 0.993 meV. The 3 meV high-energy shift with respect to the PL maximum is attributed to the thermal carrier distribution. The second resonance at 1.009 eV in the PLE spectrum is attributed to ground state absorption of smaller QDs, for which a lower lying excited state transition is resonant to the detection energy.

For the PLE spectrum of the ground state transition (panel (a)) and the PL spectrum excited in the ground state transition (panel (b)) the roles of excitation and detection are reversed. PLE probes the excited state absorption spectrum, but might be modified by restricted carrier relaxation processes and carrier localization at defects, whereas the PL spectrum is given by the absorption spectrum modified by the thermal carrier distribution among the excited states. The "absorption" spectrum extracted by multiplication of the resonantly excited PL spectrum with $\exp((E_{exc} - E_{det})/kT)$ (dotted spectrum in panel (a)) reproduces the PLE spectrum detected on the ground state transition. Obviously, the ground state absorption and emission energies are perfectly matched for the self-organized InAs/GaAs QDs, demonstrating the intrinsic nature of the exciton recombination. Additionally, for the investigated sample the PLE spectrum obviously represents the absorption spectrum of a sub-ensemble of the QDs defined by the ground state transition energy. For the self-organized InAs/GaAs QDs the excited state spectrum for a given ground state transition energy is still inhomogeneously broadened as a result of size (volume) *and* shape variations of the QDs. In the investigated samples the FWHMs of the excitation resonances are typically ≥10 meV.[19] The fact that inelastic phonon scattering is able to establish a local equilibrium state in the QDs has been established for temperatures above ~200K. However, the probability of phonon scattering processes decreases at lower temperatures,[30] possibly preventing a local equilibrium. The PLE spectra in Fig. 1b show that the shape of the near resonant excitation is practically unchanged between 7 and 200K, suggesting carrier scattering between the different localized QD states to be faster than recombination processes even at low temperatures.

Figure 6 shows for the 3.00 ML sample a contour plot of the PL intensity as a function of the detection energy and the excess excitation energy $\Delta E = E_{exc} - E_{det}$ at 7K. The PL intensity is given on a logarithmic scale. For the various excitation resonances the energy shift ΔE depends clearly on the detection energy and, therefore, the QD size. ΔE corresponds to the combined excited state splittings of the involved electron and hole states. Thus, the blue shift of ΔE with increasing detection energy demonstrates the quantum-size effect of the excited state splitting for the self-organized InAs/GaAs QDs, supporting the notion of the PLE spectra revealing the absorption spectrum. The only exemption is the resonance at ~35 meV, for which ΔE is independent of the detection energy. The intensity of this peak follows the QD ground state PL spectrum, supporting an attribution to LO-phonon assisted absorption.[31]

The PLE spectra of the 3.00 ML sample reveal for QDs with a ground state transition energy of 1.028 eV, corresponding to the maximum of the nonresonantly excited PL peak, excited state transitions about 22.5, 56.9, 76.5, 129.1, 160.7, ... meV above the ground state transition. Additional

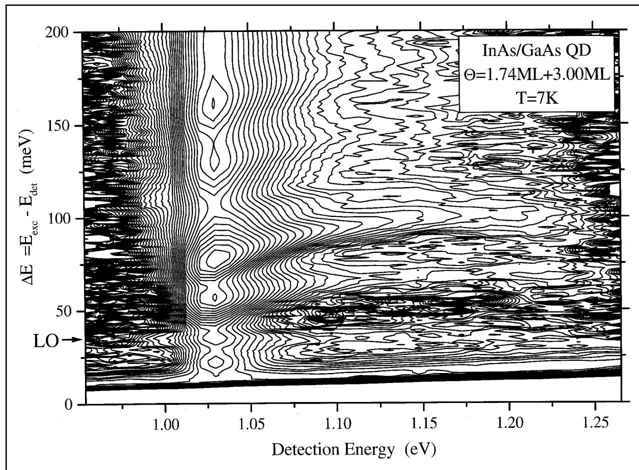

Fig. 6. Contour plot of the PL intensity in the 3.00 ML sample as a function of the detection energy and the excess excitation energy $\Delta E = E_{exc} - E_{det}$. The intensity is given on a logarithmic scale.

resonances are resolved for smaller QDs in the ensemble, see Fig. 6. The excited state transition spectrum of the QDs is, therefore, denser than expected from the inhomogneously broadened PL spectra at high-excitation densities or increased temperatures. Numerical calculations for pyramidal InAs/GaAs QDs with a base length between 10 and 20 nm and {101} sidewalls[24] indicate a variety of bound electron and hole states. Absorption spectra calculated based on these wavefunctions show transitions between a variety electron and hole levels to have sufficient oscillator strength to be observed in experiments. The low symmetry of such strained QDs leads to a breakdown of the $\Delta n = 0$ selection rule, although the most intense transitions are those with almost matching "quantum numbers" of the electron and hole wavefunctions.[24] We remind, that in the 3.00 ML sample the QDs are grown on top of smaller seed islands, which might influence their properties. Nevertheless, the calculations give a reasonable qualitative agreement with the experimentally observed excited state spectrum. The resonance at ~22.5 meV is correspondingly attributed to a transition between the electron ground state and the second excited hole state. At higher energies transitions involving excited electron states contribute to the spectrum. In fact, the calculations indicate that the inhomogeneous broadening of the excited state transitions masks a complex fine structure of the PLE resonances.

CONCLUSIONS

We have investigated the carrier capture, escape, and recombination processes in self-organized InAs/GaAs QDs as a function of temperature and excitation energy. The results evidence that the quenching of the PL intensity observed for nonresonant excitation reflects the temperature-dependence of the carrier capture process rather than thermal escape from the ground state. Thermal evaporation of carriers out of the QD ground state becomes important only for temperatures above ~200K, determining the estimated room temperature exciton lifetimes of some 10 ps, which depends on the QD size. For uniform QD ensembles the intrinsic properties of single QDs dominate: The ground state transition energy is described well by Varshni's formula and the FWHM reveals a slight increase with increasing temperature due to the population of excited hole states. An upper limit of ~4 meV is determined for the room-temperature homogeneous FWHM of the QDs. For nonuniform QD ensembles the inhomogeneity of the QD properties determines the temperature behavior. Exploiting the thermalization of carriers within each QD, we demonstrate size-selective excitation via the ground state absorption and show the intrinsic nature of the exciton recombination. PLE spectra reveal the excited state spectrum as well as its quantum-size effect in dependence on the QD ground state transition energy. The excited state spectrum is found to be much richer than suggested by high-density and high temperature PL spectra.

The experimental results for the investigated self-organized InAs/GaAs QDs show unambiguously that for each QD a local equilibrium distribution is achieved. However, thermal induced escape of carriers does not lead to the formation of a position-independent Fermi-level. The decreasing carrier capture probability and, probably, increasingly efficient nonradiative recombination in the barrier prevent an efficient redistribution of excitons in the QD ensemble. Incorporation of the QD layer in a suitable double heterostructure, keeping the carriers in the vicinity of the QDs, might improve the room-temperature PL yield.

ACKNOWLEDGMENT

Parts of this work were supported by the U.S. Air Force Office of Scientific Research, the U.S. Office of Naval Research, and the Deutsche Forschungsgemeinschaft in the framework of Sonderforschungsbereich 296.

REFERENCES

1. For a recent review see: D. Bimberg, M. Grundmann and N.N. Ledentsov, *Quantum Dot Heterostructures* (London: J. Wiley & Sons, 1999).
2. D. Leonard, K. Pond and P.M. Petroff, *Phys. Rev. B* 50, 11687 (1994).
3. J.M. Moison, F. Houzay, F. Barthe, L. Leprince, E. Andre and O. Vatel, *Appl. Phys. Lett.* 64, 196 (1994).
4. Q. Xie, P. Chen, A. Kalburge, T.R. Ramachandran, A. Nayfonov, A. Konkar and A. Madhukar, *J. Cryst. Growth* 150, 357 (1995).
5. N.P. Kobayashi, T.R. Ramachandran, P. Chen and A. Madhukar, *Appl. Phys. Lett.* 68, 3299 (1996).
6. N. Kirstaedter, N.N. Ledentsov, M. Grundmann, D. Bimberg, U. Richter, S.S. Ruvimov, P. Werner, J. Heydenreich, V.M. Ustinov, M.V. Maximov, P.S. Kop'ev and Zh.I. Alferov, *Electron. Lett.* 30, 1416 (1994); D. Bimberg, N. Kirstaedter, N.N. Ledentsov, Zh.I. Alferov, P.S. Kop'ev and V.M. Ustinov, *IEEE Sel. Topics Quant. Electron.* 3, 196 (1997).
7. Q. Xie, A. Kalburge, P. Chen and A. Madhukar, *IEEE Photon. Technol. Lett*. 8, 965 (1996).

8. O. Schmidt, N. Kirstaedter, N.N. Ledentsov, M.-H. Mao, D. Bimberg, V.M. Ustinov, A.Y. Egorov, A.E. Zhukov, M.V. Maximov, P.S. Kop'ev and Z.I. Alferov, *Electron. Lett.* 32, 1302 (1996).
9. M. Grundmann and D. Bimberg, *Phys. Rev. B* 55, 9740 (1997); *Jpn. J. Appl. Phys.* 36, 4181 (1997).
10. H. Benisty, C.M. Sotomayor Torres and C. Weisbuch, *Phys. Rev. B* 44, 10945 (1991).
11. G. Wang, S. Fafard, D. Leonard, J.E. Bowers, J.L. Merz and P.M. Petroff, *Appl. Phys. Lett*. 64, 2815 (1994).
12. W. Yang, R.R. Lowe-Webb, H. Lee and P.C. Sercel, *Phys. Rev. B* 56, 13314 (1997).
13. K. Mukai, N. Ohtsuka and M. Sugawara, *Appl. Phys. Lett.* 70, 2416 (1997).
14. F. Adler, M. Geiger, A. Bauknecht, D. Haase, P. Ernst, A. Dörnen, F. Scholz and H. Schweizer, *J. Appl. Phys.* 83, 1631 (1998).
15. Z.Y. Xu, Z.D. Lu, X.P. Yang, Z.L. Yuan, B.Z. Zheng, J.Z. Xu, W.K. Ge, Y. Wang, J. Wang and L.L. Chang, *Phys. Rev. B* 54, 11528 (1996).
16. D.I. Lubyshev, P.P. Gonzales-Borrero, E. Marega, E. Petitprez, N. La Scala and P. Basmaji, *Appl. Phys. Lett*. 68, 205 (1996).
17. M. Grundmann, R. Heitz, D. Bimberg, J.H.H. Sandmann and J. Feldmann, *phys. status solidi (b)* 203, 121 (1997).
18. R. Heitz, M. Veit, N.N. Ledentsov, A. Hoffmann, D. Bimberg, V.M. Ustinov, P.S. Kop'ev and Zh.I. Alferov, *Phys. Rev. B* 56, 10435 (1997).
19. R. Heitz, A. Kalburge, Q. Xie, M. Grundmann, P. Chen, A. Hoffmann, A. Madhukar and D. Bimberg, *Phys. Rev. B* 57, 9050 (1998).
20. N.N. Ledentsov, M. Grundmann, N. Kirstaedter, J. Christen, R. Heitz, J. Böhrer, F. Heinrichsdorff, D. Bimberg, S.S. Ruvimov, P. Werner, U. Richter, U. Gösele, J. Heydenreich, V.M. Ustinov, A. Yu. Egorov, M.V. Maximov, P.S. Kop'ev, and Zh.I. Alferov, *Proc. 22nd Intl. Conf. on the Physics of Semiconductors,* Vancouver, Canada, 1994 ed. D.J. Lockwood), Vol. 3, (Singapore: World Scientific, 1995), p. 1855.
21. M.J. Steer D.J. Mowbray, W.R. Tribe, M.S. Skolnick, M.D. Sturge, M. Hopkinson, A.G. Cullis, C.R. Whitehouse and R. Murray, *Phys. Rev. B* 54, 17738 (1997).
22. I. Mukhametzhanov, R. Heitz, J. Zeng, P. Chen and A. Madhukar, *Appl. Phys. Lett.* 73, 1341 (1998).
23. R. Heitz, I. Mukhametzhanov, P. Chen and A. Madhukar, *Phys. Rev. B* 58, R10151 (1998).
24. O. Stier, M. Grundmann and D. Bimberg, to be published in *Phys. Rev. B* 59, 5688 (1999).
25. M. Grundmann, J. Christen, N.N. Ledentsov, J. Böhrer, D. Bimberg, S.S. Ruvimov, P. Werner, U. Richter, U. Gösele, J. Heydenreich, V.M. Ustinov, A. Yu. Egorov, A.E. Zhukov, P.S. Kop'ev, and Zh.I. Alferov, *Phys. Rev. Lett*. 74, 4043 (1995).
26. K. Ota, N. Usami and Y. Shiraki, *Phys. E* 2, 573 (1998).
27. Y.P. Varshni, *Phys*. 34, 149 (1967).
28. D. Bimberg, M. Sondergeld and E. Grobe, *Phys. Rev. B* 4, 3451 (1971).
29. W. Yang, R.R. Lowe-Webb, H. Lee and P.C. Sercel, *Phys. Rev. B* 56, 13314 (1997).
30. B. Ohnesorge, M. Albrecht, J. Oshinowo, A. Forchel and Y. Arakawa, *Phys. Rev. B* 54, 11532 (1996).
31. R. Heitz, I. Mukhametzhanov, O. Stier, A. Madhukar and D. Bimberg, to be published.